nature nanotechnology

SUPPLEMENTARY INFORMATION

DOI: 10.1038/NNANO.2014.313

Nanoscale NMR spectroscopy and imaging of multiple nuclear species

Stephen J. DeVience, Linh M. Pham, Igor Lovchinsky, Alexander O. Sushkov, Nir Bar-Gill, Chinmay Belthangady, Francesco Casola, Madeleine Corbett, Huiliang Zhang, Mikhail Lukin, Hongkun Park, Amir Yacoby, and Ronald L. Walsworth

Supplementary Methods

Diamond samples:

The diamond for single NV measurements of PFOS/POSF was a $2 \times 2 \times 0.4$ mm 99.999% ^{12}C high-purity chemical vapor deposition (CVD) chip from Element 6 with an unpolished surface, implanted with 2.5-keV $^{14}N^{+}$ ions and annealed at 900 °C for 8 hours. The NV centre used for the NV NMR measurements shown in Fig. 2 of the main text was in a region with a 2D NV density of 8×10^{7} cm^{-2}, and its Hahn-echo T_2 was 26 μs.

The diamond for single NV measurements of Fomblin was a $4 \times 4 \times 0.5$ mm 99.999% ^{12}C high-purity chemical vapor deposition (CVD) chip from Element 6 with an unpolished surface, implanted with 2-keV $^{15}N^{+}$ ions at a dose of 1×10^{9} cm^{-2}. It was annealed at 800 °C for 8 hours and cleaned in a three-acid mixture (1:1:1 nitric:sulfuric:perchloric acids).

The diamond for NV ensemble measurements was a $4 \times 4 \times 0.3$ mm 99.6% ^{12}C CVD chip from Element 6 implanted with 6 keV $^{14}N^{+}$ ions at a dose of 2×10^{13} cm^{-2}. The diamond was annealed at 800 °C for 2 hours, producing NV centres with a 2D density of 3.5×10^{11} cm^{-2} in a $\sim$ 10 nm thick layer at an average depth of $\sim$ 10 nm, estimated by Monte Carlo simulations. The ensemble Hahn-echo T_2 was 3 μs.

SiO_2 structure:

The diamond used for NV ensemble NMR imaging (Fig. 4 of the main text) was prepared by cleaning in piranha solution (2 parts H_2SO_4 to 1 part H_2O_2 v/v) for more than 1 hour. Using atomic layer deposition (ALD, Savannah Atomic Layer Deposition S200), a 3 nm layer of Al_2O_3 was grown on the diamond surface followed by a 90 nm layer of SiO_2. The Al_2O_3 is necessary to achieve strong adhesion of the SiO_2 to the diamond surface and to minimize the creation of pinholes. The deposition temperature of the substrate was 250 °C, and deposition rate was 0.5 nm/min. The SiO_2-coated diamond was cleaned with acetone and isopropanol and then baked for 2 minutes on a hot plate at 115 °C to remove water. The

DOI: 10.1038/NNANO.2014.313

diamond was then spin coated with hexamethyldisilazane followed by photoresist S1805 and once again heated at 115 °C for 90 seconds. It was exposed with a photomask using a Suss MicroTec MJB4 and developed with CD26 for 45 seconds, rinsed with deionized water, and blown dry with nitrogen. SiO_2 was etched with buffered oxide etchant (BOE) for 1 minute at an etch rate of 330 nm/min. Photoresist was then removed by soaking in acetone for 5 minutes. Finally, the diamond was cleaned in piranha solution for 1 hour.

Fluorine samples:

The PFOS sample was prepared by mixing 2 mmol of solid sodium hydroxide with 2 mmol of liquid perfluorooctanesulfonyl fluoride (POSF) (Sigma Aldrich, St. Louis, MO) to produce a mixture containing sodium perfluorooctanesulfonate (PFOS). The resulting mixture was applied to the diamond surface and allowed to dry, leaving a solid sample of PFOS on the surface. For measurements of the protonated surface layer, Fomblin Y HVAC 140/13 oil was applied directly to the diamond surface.

Confocal microscope:

Measurements of PFOS/POSF with single NV centres (Fig. 2 of the main text) were performed using a custom-built scanning confocal microscope. Optical excitation was provided by an 800 mW 532 nm diode pumped solid-state (DPSS) laser (Changchun New Industries Optoelectronics Tech MLLIII532-800-1) focused onto the diamond using a 100×, 1.3 NA oil immersion objective (Nikon CFI Plan Fluor 100× oil). The laser power incident on the sample was 0.5 mW. The excitation laser was pulsed by focusing it through an acousto-optical modulator (Isomet 1205C-2). NV fluorescence was collected through the same objective and separated from the excitation beam using a dichroic filter (Semrock LM01-552-25). The light was additionally filtered (Semrock LP02-633RS-25) and focused onto a single-photon counting module (Perkin-Elmer SPCM-ARQH-12). Microwaves were delivered to the diamond using a 900 μm-diameter loop fabricated on a glass cover slip, with the diamond glued to the cover slip and in contact with the loop. The loop was driven by an amplified (Mini-circuits ZHL-16W-43-S+) microwave synthesizer (Windfreak SynthNV). The phase of microwave pulses was controlled using an in-phase/quadrature (IQ) mixer (Marki IQ1545LMP). Microwave and optical pulses were controlled using a computer-based digital delay generator (SpinCore PulseBlaster ESR400). Measurement protocols (pulse sequences, data acquisition, etc.) were controlled by custom software. The static magnetic field was applied with a permanent magnet whose distance and position relative to the NV centre was controlled

with a three-axis stage.

Measurements of Fomblin with single NV centres (Fig. 5 of the main text) were performed with a similar confocal microscope in which microwave pulses were generated with a Tektronix AFG3052C arbitrary waveform generator. Phase was controlled with an IQ mixer driven by a second Tektronix AFG3052C AWG. Microwaves were delivered via a stripline fabricated on a glass coverslip and placed against the diamond surface.

Wide-field microscope:

Measurements with NV ensembles were performed using a custom-built wide-field microscope. Optical excitation was provided by a 3W 532 nm LaserQuantum mpc6000 laser focused through a glass coverslip and the diamond chip onto the opposite diamond surface, containing the shallow, high-density NV layer, by a 100× 0.9 NA air objective (Olympus MPlan N). The laser power incident on the sample was 800 mW. The diamond was attached to the coverslip with Norland Blocking Adhesive 107 (Norland, Cranbury, NJ), which was cured under a UV lamp for 30 minutes. The laser was controlled with an acousto-optical modulator (Isomet M1133-aQ80L-1.5). The NV fluorescence signal was collected through the same objective and separated from the excitation beam with a dichroic mirror (Semrock LM01-552-25) and optical filters (Semrock LP02-633RS-25 and FF01-750SP-25) before being imaged onto a CCD camera (Starlight Express SXVR-H9). An optical chopper was used to block fluorescence during optical state preparation of the NV centres. Microwaves were synthesized with a signal generator (Agilent E8257D), amplified (Mini-circuits ZHL-16W-43-S+), and applied to the sample with a small wire loop placed against the diamond. The microwave pulse phase was controlled by an IQ mixer (Marki IQ1545LMP). Microwave and optical pulses were controlled by a pulse generator (SpinCore PulseBlasterESR-PRO 500 MHz) governed by custom software. The static magnetic field was applied with a permanent magnet whose distance and position relative to the NV ensemble was controlled with a three-axis stage.

The laser spot on the diamond had a FWHM size of $\sim$ 60 μm. For the white light images, each CCD pixel represented 200 nm x 200 nm on the diamond surface. For the NV fluorescence measurements, each CCD pixel represented 1 x 1 μm on the diamond surface, although the point spread function of the detection optics was $\sim$ 500 nm. Smaller CCD pixels could be used, with reduced SNR. Each NV NMR measurement average was performed for 500 ms (2000 chopper cycles) at each dynamical decoupling delay, and a full

DOI: 10.1038/NNANO.2014.313

dataset consisted of $\sim$ 800 averages. For simple spectroscopic measurements, a 26 μm x 20 μm field of view was sampled and the measurements from each pixel were averaged together before further processing. For imaging, a larger field of view was sampled and each pixel was analyzed separately. For display, as in Fig. 4b of the main text, the image was further processed with a 3-pixel width Gaussian blur as a way to bin pixels smoothly and improve the SNR of the pixel-by-pixel spectra. For each pixel, the NV NMR contrast of the fluorine dip was calculated by fitting the spectrum with two Lorentzian curves, one for fluorine and one for protons. Each pixel was then assigned a color, blue for a fluorine contrast value below a threshold indicating ^{19}F, red for a contrast above a threshold indicating no ^{19}F, or an intermediate color for values between the thresholds. The thresholds were determined by the contrast needed to distinguish the ^{19}F signals from the noise.

NV NMR measurements, spectral model, and NV depth estimation:

Spin-state measurements take place in the NV ground electronic state, in which the $|0\rangle$ spin state is split from $|1\rangle$ and $|-1\rangle$ spin states by a zero-field splitting of 2.87 GHz, and $|1\rangle$ and $|-1\rangle$ experience Zeeman splitting in the presence of an external magnetic field. NV fluorescence is induced with a 532 nm laser pulse, with a stronger signal when spins are in state $|0\rangle$, as well as optical pumping into $|0\rangle$, due to non-radiative decay from the $|1\rangle$ and $|-1\rangle$ excited electronic states through metastable singlet states and then into $|0\rangle$.

For the NV NMR experiments described here, the magnetic signal of interest is produced by nuclear spins on the diamond surface interacting with shallow NV centres through magnetic dipole-dipole coupling. The specific components of the dipole-dipole Hamiltonian that are responsible for the measured signal stem from the $S_z I_x$ and $S_z I_y$ terms, where S_z is the z component of the NV spin (defined by the NV symmetry axis) and $I_{x,y}$ are the x and y components of the nuclear spin. These terms couple the NV spin to the transverse component of the nuclear spin, which precesses in a static magnetic field at the nuclear Larmor frequency. A nearby permanent magnet aligned with the NV centre quantization axis sets the static magnetic field, B_0. A single measurement consists of repeating the optical pumping, XY8-k sequence, and optical detection a few hundred times in order to collect sufficient photons at the detector. The measurement is then repeated for a series of XY8-k pulse delay times, τ, to determine the spectrum of the magnetic environment. When τ matches a half-period of the nuclear spin precession, the magnetic coupling effectively drives the NV spin away from the initial spin state, which is detected as a change in NV fluorescence intensity. These dips

in the signal occur at the Larmor frequencies of nuclei on the surface (or other sources of noise, such as nuclear impurities within the diamond).

To perform NV NMR measurements, two fluorescence measurements F_1 and F_2 were acquired for each pulse sequence delay with the final $\pi/2$ pulse 180° out of phase. This procedure removes common-mode noise from laser intensity fluctuations. Normalized contrast, C, was then calculated as

$$C = \frac{F_2 - F_1}{F_2 + F_1}. \tag{S1}$$

Note that for wide-field microscope measurements, this normalization was performed pixel-by-pixel. The signal-to-noise ratio of a single measurement is small due to low optical collection efficiency and the relatively short NV T_2. To achieve an SNR > 3, several hundred individual contrast measurements were typically averaged together. The broad decrease in contrast resulting from intrinsic NV decoherence is fully described by a stretched exponential, but was removed during data analysis with a linear baseline correction, which is an acceptable approximation over the small range of delay times scanned. The corrected contrast was fit with the function

$$C(\omega) = \exp\left(-\sum_i \chi_i(\omega)\right), \tag{S2}$$

where $\chi_i(\omega)$ describes the NV decoherence due to each nuclear species, i. It is a function of the frequency-dependent variance in the magnetic field signal (spectral density), $\langle|B_z^i(\Omega, \omega_{L,i})|^2\rangle$, created by the nuclear spins, as well as a function $G(\Omega, \tau, N)$ describing the NV sensor response to the pulse sequence. For the time-domain measurements,

$$\chi_i(\tau) = \frac{\gamma_e^2}{4\pi}\int_{-\infty}^{+\infty}\left\langle\left|B_z^i(\Omega, \omega_{L,i})\right|^2\right\rangle |G(\Omega, \tau, N)|^2 \, \mathrm{d}\Omega. \tag{S3}$$

Here, Ω is a dummy variable for frequency. The function $G(\Omega, \tau, N)$ is the Fourier transform of $g(t)$, where $g(t)$ is a function describing the sign of NV spin phase accumulation during the pulse sequence. For the primary resonance of the XY8-k sequence,

$$|G(\Omega, \tau, N)|^2 \approx \frac{4}{\pi^2}(N\tau)^2 \mathrm{sinc}^2\left(\frac{N\tau}{2}\left(\Omega - \frac{\pi}{\tau}\right)\right). \tag{S4}$$

The magnetic signal created by a semi-infinite layer of spin-1/2 nuclei with density ρ near an NV centre oriented along the [1 1 1] crystallographic axis is

$$\langle|B_z(\Omega, \omega_L)|^2\rangle = \rho\frac{5\pi}{48}\left(\frac{\mu_0\hbar\gamma_n}{4\pi}\right)^2\left(\frac{1}{(d_{NV} + z_1)^3} - \frac{1}{(d_{NV} + z_2)^3}\right)\frac{T_2^{*-1}}{(\Omega - \omega_L)^2 + (T_2^{*-1})^2}, \tag{S5}$$

DOI: 10.1038/NNANO.2014.313

where ω_L is the nuclear Larmor frequency, T_2^* is the nuclear spin dephasing time, d_{NV} is the depth of the NV centre below the diamond surface, z_1 is the distance from the diamond surface to the lower bound of the layer, and z_2 is the distance from the diamond surface to the upper bound of the layer. Combining these expressions and using the relationship $\omega = \pi/\tau$ for the filter resonance condition gives the frequency-domain expression

$$\chi_i(\omega) = \rho_i \frac{5}{48\pi} \left(\frac{\mu_0 \gamma_{n,i} \gamma_e \hbar}{4\pi} \right)^2 \left(\frac{1}{(d_{NV} + z_1)^3} - \frac{1}{(d_{NV} + z_2)^3} \right) I_i(\omega), \tag{S6}$$

where $I_i(\omega)$ is the convolution between the Lorentzian lineshape of the nuclear spin signal from species i and the $\mathrm{sinc}^2(\omega)$ lineshape of the filter function for the XY8-k sequence. It can be expressed as

$$I_i(\omega) = \frac{2T_{2,i}^{*2}}{\left[1 + T_{2,i}^{*2} (\omega_{L,i} - \omega)^2\right]^2} \left\{ e^{-\frac{N\pi}{\omega T_{2,i}^*}} \left[\left[1 - T_{2,i}^{*2} (\omega_{L,i} - \omega)^2\right] \cos\left[\frac{N\pi}{\omega} (\omega_{L,i} - \omega)\right] \right.\right.$$
$$\left.\left. - 2T_{2,i}^* (\omega_{L,i} - \omega) \sin\left[\frac{N\pi}{\omega} (\omega_{L,i} - \omega)\right] \right] - 1 + \frac{N\pi}{\omega T_{2,i}^*} \left[1 + T_{2,i}^{*2} (\omega_{L,i} - \omega)^2\right] + T_{2,i}^{*2} (\omega_{L,i} - \omega)^2 \right\}, \tag{S7}$$

where $N = 8k$ is the total number of π-pulses. For additional details see Supplementary Ref. 2.

To estimate the depth of single NV centres, NV NMR measurements were performed with a drop of immersion oil (Olympus Type-F Low Auto-Fluorescence) on the diamond surface. The parameters ω_L, d_{NV}, and T_2^* were determined by fitting the NV NMR signal contrast with equation (S2) using a density[1] $\rho = 60$ protons/nm^3 and assuming $z_1 = 0$ and $z_2 \to \infty$. Nonlinear fitting was performed using an iterative least squares method implemented with MATLAB.

To calculate the thickness of the proton layer described in Fig. 5 of the main text, the ^{1}H and ^{19}F spectral dips were simultaneously fit using equation (2). A ^{1}H layer of finite thickness and density $\rho = 60$ protons/nm^3 was assumed to lie between the diamond and a semi-infinite layer of Fomblin Y oil with density $\rho = 40$ fluorines/nm^3. The proton layer thickness, t, and NV depth, d, were left as free parameters determined by fitting. The noise spectrum of both the Fomblin oil and the proton layer were assumed to be given by delta-functions in frequency space. By observing the scaling of the NMR signals with the number of applied pulses, both nuclear dephasing timescales were determined to be much longer

than those probed in this experiment. Also tested was an alternative model in which both ^{1}H and ^{19}F were isotropically distributed in a semi-infinite layer on the diamond surface. For the two NV centres at different depths described in Fig. 5 of the main text, it was found that the ratio of ^{1}H:^{19}F in the sample would need to vary by a factor of two to achieve a similar goodness of fit as the thin-layer model. This large ^{1}H:^{19}F variation was inconsistent with the fact that the NVs, spaced only 5 μm apart, were interrogating the same sample, and so this hypothesis was rejected. Similar results, consistent only with the thin-layer model, were found for other proximal NV centres in other regions of the diamond (see Fig. S1).

Supplementary Figure

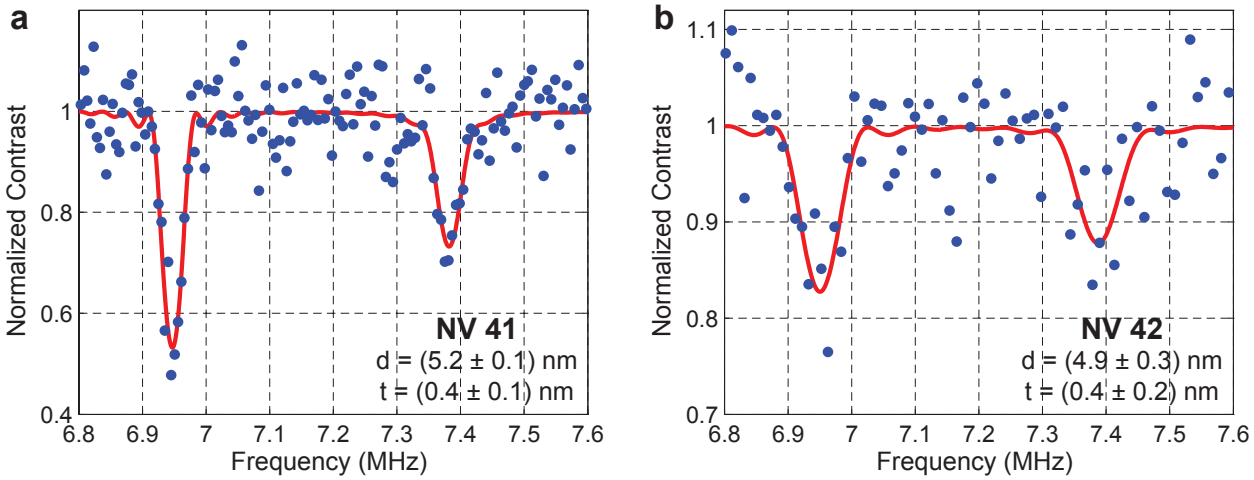

FIG. S1. **Determination of surface proton layer thickness.** NMR signal from Fomblin Y oil on the diamond surface measured with two NV centres at a different location from those in the main text. NV depths (d) and layer thickness (t) are presented, as calculated from the lineshape model (see Supplementary Methods).

Supplementary References

[1] Loretz, M., Pezzagna, S., Meijer, J. & Degen, C. L. Nanoscale nuclear magnetic resonance with a 1.9-nm-deep nitrogen-vacancy sensor. *Applied Physics Letters* **104**, 033102 (2014).

[2] Pham, L. M., *et al.* Technique for measuring nitrogen-vacancy center depth in diamond. *Submitted to Physical Review B.*